Inorganic Chemistry

Article

pubs.acs.org/IC

Dicyanogermylenes: A Tale of Isomers and Interconversions

Ashwini Bundhun,[†] Hassan H. Abdallah,[‡,⊥] Ponnadurai Ramasami,*[,†] Peter P. Gaspar,[§] and Henry F. Schaefer, III*[,∥]

[†]Computational Chemistry Group, Department of Chemistry, University of Mauritius, Réduit, Mauritius

[‡]School of Chemical Sciences, Universiti Sains Malaysia, Penang, Malaysia 11800

[§]Department of Chemistry, Washington University, Saint Louis, Missouri 63130, United States

[∥]Center for Computational Quantum Chemistry, University of Georgia, Athens, Georgia 30602, United States

Supporting Information

ABSTRACT: A systematic investigation is carried out using the B3LYP, BLYP, and BHLYP functionals and MP2 level of theory to characterize the low-lying electronic singlet and triplet GeC_2N_2 isomers. The basis sets used are of double-ζ plus polarization quality with additional s- and p-type diffuse functions, DZP++. Three bent isomers $Ge(CN)_2$, CNGeCN, and $Ge(NC)_2$ are located on the singlet and triplet potential energy surfaces. In visualizing the reaction pathways for the singlet isomerization of the bent isomers, two three-membered [Ge, C, N] cyclic systems, with exocyclic −C−C≡N and −C−N≡C bonding, appear on the energy surface. Four types of electron affinities reported are: the adiabatic electron affinity, the zero-point vibrationally corrected electron affinity, the vertical electron affinity, and the vertical detachment energy of the anion. The ionization energies and singlet−triplet gaps for all isomers are also reported. The energetic ordering (kcal mol^{-1}) (B3LYP) with zero-point vibrational energy corrections for the singlet ground state isomers follows: $Ge(CN)_2$ (global minimum) < CNGeCN (2.3) < $Ge(NC)_2$ (3.3) < Cyc_exo_CCN (15.3) < Cyc_exo_CNC (30.6). All the bent and cyclic isomers are found to be below the dissociation limit to Ge (^{3}P) + C_2N_2 ($^1\Sigma_g$). The rate constants for all interconversions are evaluated using transition state theory.

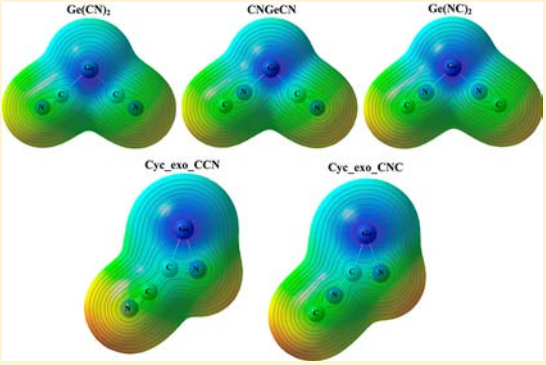

I. INTRODUCTION

The quest for novel dicyanogermylenes is a promising area of active research following spectacular progress in the exploration of cyano/isocyano derivatives of carbenes[1−5] and silylenes.[6,7] Germanium-containing species are essential in the microelectronic industry in the form of wafers,[8] semiconductors,[9] and dielectrics.[10]

Several experimental[11−17] and theoretical[18−20] investigations have been reported for cyanogen derivatives since 1977. A number of researchers have focused on the isomers of cyanomethylene, HCCN,[21−35] to determine their equilibrium geometries. The mass spectrometric observation of dicyanocarbene, $C(CN)_2$ was reported by Schwarz et al.[36] Early theoretical studies of $C(CN)_2$ included those of Hoffmann et al.[37] and Lucchese and Schaefer.[38] In the latter study the triplet state was estimated to lie ∼14 kcal mol^{-1} below its singlet state. By means of anion photoelectron spectroscopy, Wenthold et al.[39] reported dicyanocarbene as a triplet ground state, and the adiabatic electron affinity of NCCCN was measured to be 3.72 ± 0.02 eV, while the singlet−triplet splitting was estimated to be 0.52 ± 0.05 eV.

Chaudhuri et al.[40] reported a theoretical study of the ground and excited states of the isomers of C_3N_2. The relative energies of the electronic states of dicyanocarbene and its negative ion and of cyclic C_3N_2 were predicted to follow the order X ^{1}A′ < X $^1A_1$ < 1 $^3B_1$ < X $^3\Sigma_g^-$ < X $^2B_1$. Hajgató et al.[41] characterized the energies of the isomers as $C(CN)_2$ < CNCCN < $C(NC)_2$, irrespective of the electronic state. The adiabatic ionization energies were estimated as: $C(CN)_2$ = 11.3 eV to the linear $^2\Pi_u$ cation; NCCNC = 10.4 eV to the linear $^2\Pi$ cation and $C(NC)_2$ = 9.9 eV to the bent $^2A_1$ cation. Maier and Reisenauer[42] calculated the geometries and relative energies of C_3N_2 isomers in their singlet and triplet states, and the global minimum was located as triplet linear $C(CN)_2$ ($D_{\infty h}$, $^3\Sigma_g^-$). Maier et al.[43] also studied five C_2N_2Si isomers pertinent to the reaction Si (^{3}P) + N≡C−C≡N ($D_{\infty h}$, $^1\Sigma_g$), identifying the bent $Si(NC)_2$ as the global minimum and the next two higher isomers as NCSiNC and $Si(CN)_2$. There are two cyclic silylenes, but the mechanism for the reorganization of the Si atom and two CN fragments is not known. Subsequently, there have been several investigations[44−48] dealing with structural isomerizations of cyano compounds.

A preliminary report of the preparation of the germanium(II) pseudohalide, $Ge(CN)_2$ and its reactions with 2,3-dimethylbutadiene, $[FeCp(CO)_2]_2$, and α,α'-bipyridine was published in 1986 by Satge and co-workers,[49] without considering questions of isomerization. More recently, the development of bulky

Received: June 8, 2012
Published: November 7, 2012

germanium isocyanide complexes succeeded.[50,51] Brown et al.[50] studied the diarylgermylene reaction $Ge(Ar^{Me}{}_6)_2$ [$Ar^{Me}{}_6$ = C_6H_3-2,6-(C_6H_2-2,4,6-$(CH_3)_3)_2$] + *tert*-butyl isocyanide → $(Ar^{Me}{}_6)_2GeCNBu^t$ (Lewis base adduct). Therein, the N−C stretching frequency of the isocyanide ligand decreases upon formation of the Lewis base adduct. This may be explained in terms of a n → π^* back-bonding interaction. Using the hybrid PBE1PBE exchange correlation functional in combination with TZVP basis sets, they confirmed the HOMO to be a Ge−C bonding combination between the lone pair of electrons on the Ge atom and the C−N π^* orbital of the isocyanide ligand.

While many rearrangements of silylenes, including those with unsaturated substituents, are well-documented,[52,53] very few rearrangements of germylenes have been reported. Grev and Schaefer[54] predicted the $HGeSiH_3 \rightleftharpoons H_2Ge{=}SiH_2$ rearrangement to be endothermic by 3.2 kcal mol^{-1}, with a barrier of 16.2 kcal mol^{-1}. For the $HGeGeH_3 \rightleftharpoons H_2Ge{=}GeH_2$ rearrangement an exothermicity of 2.0 kcal mol^{-1} was predicted to be in close agreement with the computed results obtained by Trinquier.[55] A barrier of 10.0 kcal mol^{-1} was predicted for the latter rearrangement. Khabashesku et al.[56] presented evidence for the reversible germylene-to-germene rearrangement displayed in the following reaction Scheme 1, studied in a frozen matrix.

Scheme 1. Germylene-to-Germene Rearrangement

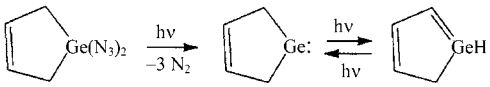

Gaspar, Lee, and Lei[57] examined the gas-phase reactions of $MeGeSiMe_3$. Germylene-to-germylene rearrangements formed $HGeCH_2SiMe_3$ and $MeGeCH_2SiHMe_2$ via a three-membered ring intermediate resulting from carbon−hydrogen bond insertion by the germylene center into a C−H bond of the trimethylsilyl group. No products were found that demanded the rearrangement of $MeGeSiMe_3$ to $Me_2Ge{=}SiMe_2$.

In view of the above and following the successful experimental and theoretical findings for the isomers of C_3N_2 and SiC_2N_2, the plan for the current investigation of the isolated and interconversions of new GeC_2N_2 analogs is displayed in Scheme 2. The literature of the dicyanogermylene isomers is limited and therefore there are no experimental data for comparisons. The investigation of the gas-phase anions is particularly useful in the field of spectroscopic studies and photodissociation reactions.

II. THEORETICAL METHODS

All geometries were fully optimized with the Gaussian 03 program,[58] using three functionals, BHLYP, BLYP, and B3LYP, and the MP2 method. BHLYP is an HF/DFT hybrid method employing the Becke (B)[59] half and half exchange functional (H)[60] and the Lee, Yang, and Parr (LYP)[61] nonlocal correlation functional. The B3LYP method combines Becke's three-parameter exchange functional (B3) with the LYP correlation functional. BLYP is a pure DFT method, comprised of Becke's (B) exchange functional plus the LYP correlation. MP2[62] computations with the frozen core approximation were also performed. Natural bond orbital analyses were carried out with NBO 3.1.[63] In all cases, an extended integration grid (199 974) was used, with very tight convergence criteria applied to all computations.

Double-ζ basis sets with polarization and diffuse functions, denoted as DZP++, were used for all atoms. The double-ζ basis sets were constructed by augmenting the Huzinaga−Dunning−Hay[64−66] sets of contracted Gaussian functions with one set of p polarization functions and one set of d polarization functions for each carbon [α_d(C) = 0.75] and nitrogen [α_d(N) = 0.80] atom. The diffuse functions were determined in an even-tempered fashion following the prescription of Lee[67]

$$\alpha_{\text{diffuse}} = \frac{1}{2}\left(\frac{\alpha_1}{\alpha_2} + \frac{\alpha_2}{\alpha_3}\right)\alpha_1$$

where α_1, α_2 and α_3 are the three smallest Gaussian orbital exponents of the s- or p-type primitive functions of a given atom ($\alpha_1 < \alpha_2 < \alpha_3$). Thus α_s(C) = 0.04302, α_p(C) = 0.03629, α_s(N) = 0.06029, α_p(N) = 0.05148. The DZP++ basis set for germanium was comprised of the Schafer−Horn−Ahlrichs

Scheme 2. Ground State Structures for Bent and Cyclic Dicyanogermylenes

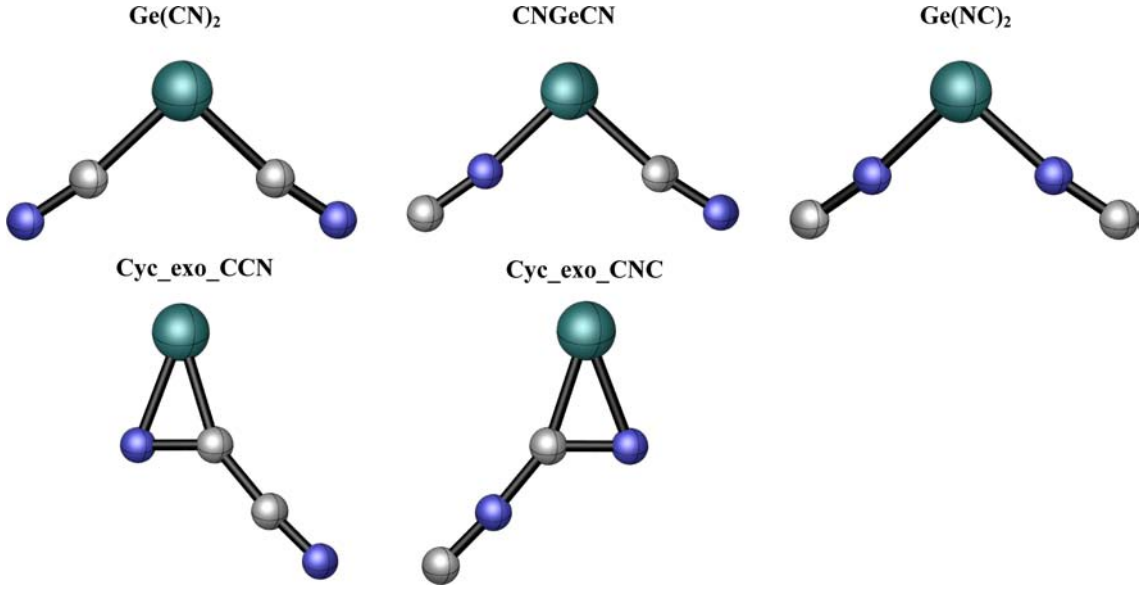

dx.doi.org/10.1021/ic301225w | Inorg. Chem. 2012, 51, 12152−12164

Table 1. Germylenes EA_{ad} and $EA_{ad(ZPVE)}$ (in Parentheses), EA_{vert}, VDE, E_{IE}, and ΔE_{S-T} (kcal mol^{-1} in Parentheses) in Electron Volts (eV)

	BHLYP	BLYP	B3LYP	MP2
		EA_{ad} ($EA_{(ZPVE)}$)		
$Ge(CN)_2$	2.73 (2.73)	2.56 (2.56)	2.78 (2.78)	2.22 (2.07)
CNGeCN	2.45 (2.45)	2.38 (2.38)	2.55 (2.56)	2.20 (2.12)
$Ge(NC)_2$	2.16 (2.16)	2.18 (2.19)	2.32 (2.32)	2.16 (2.14)
Cyc_exo_CCN	1.30 (1.33)	1.35 (1.38)	1.46 (1.49)	−0.70 (−0.71)
Cyc_exo_CNC	1.22 (1.24)	1.32 (1.34)	1.41 (1.43)	−0.74 (−0.74)
		EA_{vert}		
$Ge(CN)_2$	2.71	2.54	2.76	1.95
CNGeCN	2.37	2.32	2.49	2.00
$Ge(NC)_2$	2.04	2.10	2.22	2.00
Cyc_exo_CCN	0.41	0.84	1.34	−0.33
Cyc_exo_CNC	0.06	1.18	1.25	−0.76
		VDE		
$Ge(CN)_2$	2.76	2.58	2.80	2.37
CNGeCN	2.54	2.44	2.63	2.36
$Ge(NC)_2$	2.32	2.29	2.45	2.34
Cyc_exo_CCN	1.46	1.95	1.60	−0.68
Cyc_exo_CNC	1.42	1.51	1.59	−0.71
		E_{IE}		
$Ge(CN)_2$	10.85	10.51	10.86	10.53
CNGeCN	10.80	10.32	10.79	10.62
$Ge(NC)_2$	10.82	10.07	10.69	10.81
Cyc_exo_CCN	8.74	8.47	8.76	
Cyc_exo_CNC	8.59	8.40	8.66	8.80
		ΔE_{S-T}		
$Ge(CN)_2$	1.76 (40.6)	1.87 (43.2)	1.85 (42.7)	2.08 (48.0)
CNGeCN	2.15 (49.5)	2.16 (49.8)	2.21 (50.9)	2.18 (50.4)
$Ge(NC)_2$	2.62 (60.4)	2.44 (56.2)	2.63 (60.6)	2.46 (56.6)

double-ζ spd set plus a set of five pure d-type polarization functions with $\alpha_d(Ge) = 0.246$, augmented by a set of sp diffuse functions with $\alpha_s(Ge) = 0.024434$ and $\alpha_p(Ge) = 0.023059$.[68] The overall contraction scheme for the basis sets is: C(10s6p1d/5s3p1d), N(10s6p1d/5s3p1d), and Ge-(15s12p6d/9s7p3d).

Four forms of neutral-anion energy differences are evaluated for each structure at every level of theory.

adiabatic electron affinities

$$EA_{ad} = E(\text{optimized neutral}) - E(\text{optimized anion}) \quad (1)$$

Zero-point vibrational energies (ZPVE) were evaluated at each level.

ZPVE corrected adiabatic electron affinities $EA_{ad(ZPVE)}$

$$EA_{ad(ZPVE)} = [E(\text{optimized neutral}) + ZPVE_{neutral}] - [E(\text{optimized anion}) + ZPVE_{anion}] \quad (2)$$

vertical electron affinity

$$EA_{vert} = E(\text{optimized neutral}) - E(\text{anion at optimized neutral geometry}) \quad (3)$$

vertical detachment energy of the anion

$$VDE = E(\text{neutral at optimized anion geometry}) - E(\text{optimized anion}) \quad (4)$$

The ionization energies are computed as

$$E_{IE} = E(\text{optimized cation}) - E(\text{optimized neutral}) \quad (5)$$

Each singlet−triplet splitting was predicted as the difference between the electronic energy of the neutral ground state and that of its lowest triplet state.

Quantum chemical modeling was performed to elucidate the unimolecular isomerizations for the GeC_2N_2 molecule on the singlet and triplet PESs. All transition state (TS) searches were performed without symmetry restriction. The stationary state geometries were analyzed via harmonic vibrational frequencies and characterized as ground states or TSs. Further, intrinsic reaction coordinates (IRC) were computed using mass-weighted internal coordinates to verify the connectivity of the reactants and products.

III. RESULTS AND DISCUSSION

The energy for the Ge (^1D) + C_2N_2 ($^1\Sigma_g$) system relative to the global minimum $^1A_1$ $Ge(CN)_2$ is predicted to be 71.2 kcal mol^{-1}. As a result, all singlet and triplet equilibrium structures are energetically well below the dissociation limit Ge (^1D) + C_2N_2 ($^1\Sigma_g$), where the dissociation products are computed in their ground electronic states. The neutral closed-shell molecules $Ge(CN)_2$, CNGeCN, and $Ge(NC)_2$, their anions, cations, and the triplet excited states of the neutral species are all planar. Two cyclic systems have been identified on the singlet PES; these are also planar structures. The two important bond angles used to describe the isomers are the divalent angle (θ) and the quasi-linear Ge−C≡N or Ge−N≡C bond angles (ϕ). A remarkable feature of the divalent angles of the acyclic bent neutral singlet state isomers is the angle opening in the

dx.doi.org/10.1021/ic301225w | Inorg. Chem. 2012, 51, 12152−12164

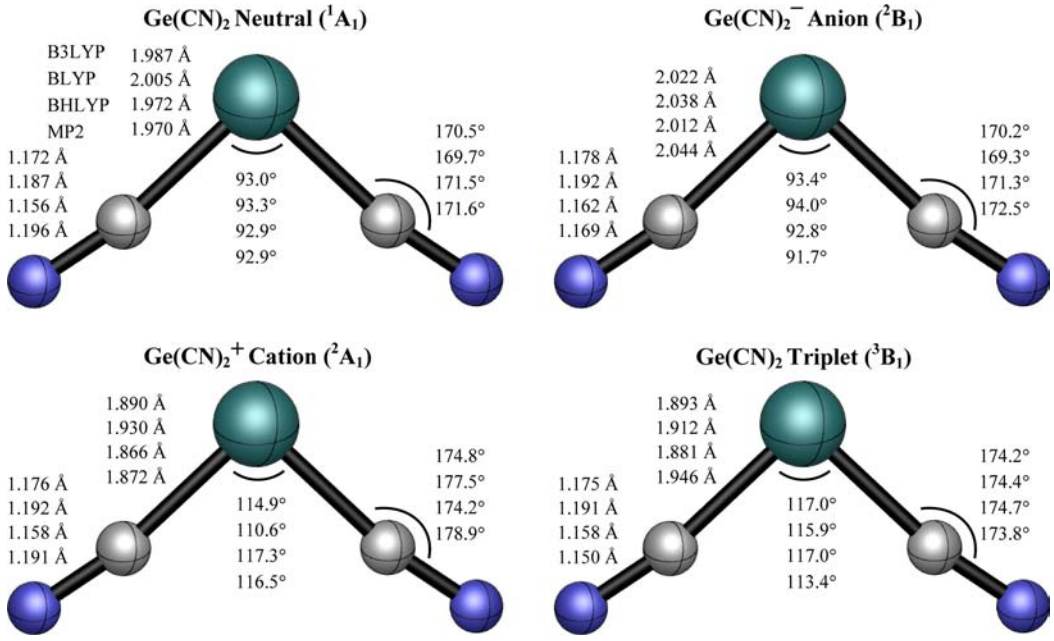

Figure 1. Equilibrium geometries for the $^1A_1$ ground state of $Ge(CN)_2$, $^2B_1$ ground state of the $Ge(CN)_2^-$ anion, $^2A_1$ ground state of the $Ge(CN)_2^+$ cation, and $^3B_1$ excited state of neutral $Ge(CN)_2$.

corresponding low-lying triplet states. This change in angle is associated with a change in the electronic configuration. Thus the corresponding cyclic systems have not been located as triplet species on the GeC_2N_2 PES. The multiplicities, identity of the electronic states and geometries of the dicyanogermylene equilibrium structures and of the isocyano, diisocyano, and cyclic germylene isomers are analyzed and compared. Table 1 presents the germylenes EA_{ad} and $EA_{ad(ZPVE)}$ (in parentheses), EA_{vert}, VDE, E_{IE}, and ΔE_{S-T} (kcal mol^{-1} in parentheses) in electron volts (eV) for all species. Supporting Information Figure S1 shows the plots of the electrostatic potentials in Hartree on the 0.001 electrons/bohr^3 charge density isodensity surface of the $Ge(CN)_2$, CNGeCN, $Ge(NC)_2$, Cyc_exo_CCN, and Cyc_exo_CNC molecules.

A. Electronic Configuration. The global minimum on the singlet PES is the $^1A_1$ ground state dicyanogermylene $Ge(CN)_2$ molecule. The lowest-lying triplet $^3B_1$ states of $Ge(CN)_2$ and $Ge(NC)_2$ of C_{2v} symmetry are singly excited states ($14a_1 \rightarrow 5b_1$) relative to the closed-shell singlets. Their electronic configurations are listed in Table S1 (Supporting Information).

For the $^1A_1$ ground state isomers of $Ge(CN)_2$ and $Ge(NC)_2$, the HOMO is of a_1-symmetry, corresponding to the lone pair of electrons lying in the molecular plane. This is a σ-type antibonding orbital having contributions from the in-plane p-orbital of the Ge atom and from the in-plane p orbitals of the pseudohalogen. In the lowest-lying $^3B_1$ triplet state, one of the two $14a_1$ electrons is promoted to an orbital of b_1-symmetry, which is the out-of-plane p-atomic orbital of the divalent germanium center. In comparison to the GeH_2 molecule,[69] the contribution of the germanium s orbital to the bonding orbital for the highly electronegative ligand C≡N is large, thus decreasing the energy of the a_1 orbital. This leads to an increase in the HOMO−LUMO gap, favoring electron pairing. Hence the singlet state is preferred.

For the $^2B_1$ ground state anion, three nonbonding electrons reside on the germylene Ge atom, with two electrons in the a_1 σ-orbital and one electron in the b_1 π-orbital. The anions are stabilized by incorporating more s orbital character into the doubly occupied orbitals which favors a bent geometry. The promotion of an ($a_1 \rightarrow b_1$) electron of one of the neutral ground states yields the neutral $^3B_1$ states with one electron in each nonbonding orbital of the Ge atom. The electronic structure of the triplet states shows that the p electrons of the Ge atom can participate in π bonding with the cyano/isocyano/diisocyano groups.

In the singlet $^1A'$ ground state CNGeCN (C_s symmetry), the HOMO is of a′ symmetry, corresponding to the lone pair of electrons lying in its molecular plane. In the triplet state a single electron is moved to a SOMO a″ orbital, which is qualitatively the out-of-plane p orbital on the divalent germanium center. The relative energies of the isomers can be addressed using valence bond theory. The energies of the $Ge(CN)_2$, CNGeCN, and $Ge(NC)_2$ isomers vary depending on the different pairing abilities of the two constituent C≡N/N≡C groups to the atomic Ge (^3P). The ·C≡N: group with an unpaired electron largely localized on the carbon atom is used as a guide to rationalize the energetic order of the different isomers of dicyanogermylene. In classifying the energetic order of these molecules, the localization of the nonbonding electron on the carbon atom of the C≡N or N≡C group proves to be decisive. The order of stabilities of the isomers are: (most stable) $Ge(CN)_2$ > CNGeCN > $Ge(NC)_2$ > Cyc_exo_CCN > Cyc_exo_CNC (least stable). The energetic ordering follows the same trend with all functionals. Supporting Information Table S2 presents the NBO population analyses for the electronic configurations of the bent isomers $Ge(CN)_2$, CNGeCN, and $Ge(NC)_2$ from the hybrid B3LYP density functional. The Ge−C≡N and Ge−N≡C moieties of the CNGeCN structure show similar bonding properties as the Ge−C≡N bonds in $Ge(CN)_2$ molecule and Ge−N≡C bonds in $Ge(NC)_2$ molecule, respectively.

i. Ge(CN)$_2$ (Figure 1). The neutral Ge−C bond lengths lie from 1.972 (BHLYP) to 2.005 Å (BLYP), respectively while the MP2 level of computation predicts shorter Ge−C bond distances of 1.970 Å. The predicted C≡N bond lengths vary from 1.156 Å (BHLYP) to 1.196 Å (MP2). The divalent angle

dx.doi.org/10.1021/ic301225w | Inorg. Chem. 2012, 51, 12152−12164

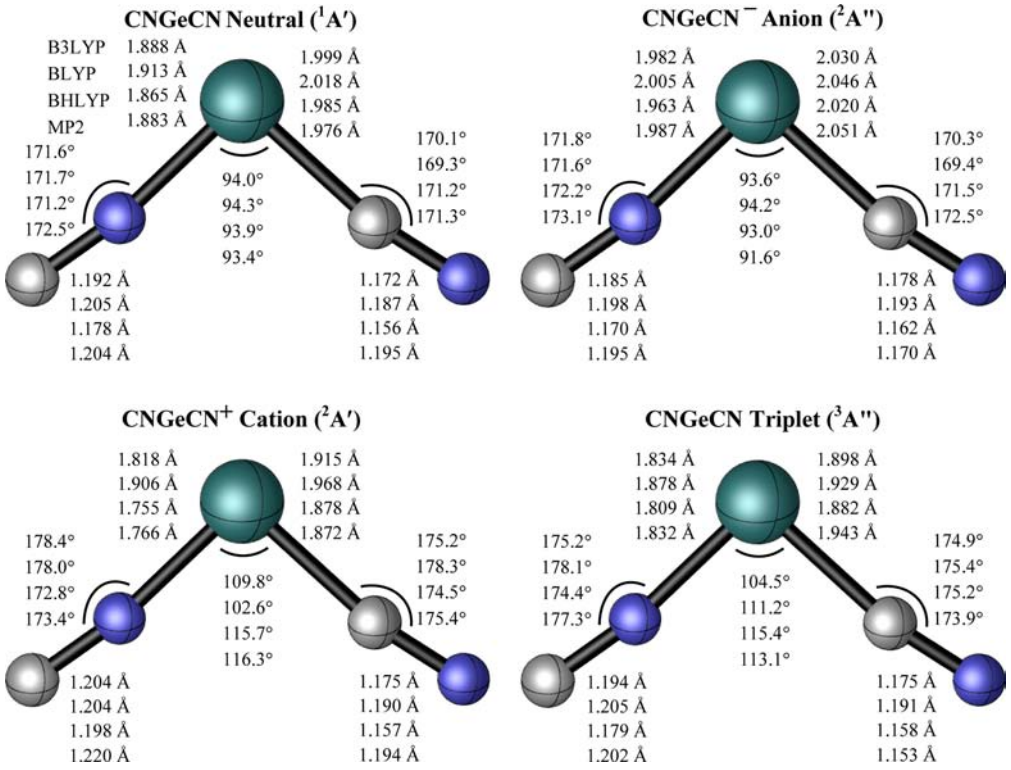

Figure 2. Equilibrium geometries for the $^1A'$ ground state of CNGeCN, $^2A''$ ground state of the $CNGeCN^-$ anion, $^2A'$ ground state of the $CNGeCN^+$ cation, and $^3A''$ excited state of neutral CNGeCN.

θ falls from 92.9° (BHLYP) to 93.3° (BLYP) and the quasi-linear bond angles ϕ(Ge−C≡N) lie from 169.7° (BLYP) to 171.6° (MP2). These values may be compared with the experimental bond lengths for Mes_3GeCN [r(Ge−C) = 1.975 Å, r(C−N) = 1.149 Å] and $Mes_2Ge(CN)_2$ [r(Ge−C) = 1.944 Å, r(C−N) = 1.121 Å] reported by Hirara et al.[51] From the singlet $^1A_1$ ground state of $Ge(CN)_2$ upon addition of an extra electron, the Ge−C anion bond distances range from 2.012 Å (BHLYP) to 2.044 Å (MP2). The C≡N bond length increases slightly at the BHLYP, BLYP, and B3LYP functionals, except at the MP2 level of computation a decrease of 0.027 Å is noted. No appreciable differences are observed in the divalent angle θ and the quasi-linear angle, ϕ, for the $^1A_1 \rightarrow {}^2B_1$ electron attachment. For the $Ge(CN)_2^+$ cation the Ge−C bond distances decrease by 0.097 Å while the C≡N bond distances increase by 0.004 Å (B3LYP) compared to the neutral counterpart. The loss of an electron from the $^1A_1$ ground state $Ge(CN)_2$ causes the divalent angle θ to increase significantly by 22° (B3LYP) or 24° (MP2), accompanying an increase in ϕ(Ge−C≡N) by 4° and 7°, respectively. In going from the $^1A_1$ to the $^3B_1$ states of $Ge(CN)_2$ the Ge−C bond length is shortened by 0.094 Å. Similarly, the C≡N bond lengthens by 0.003 Å (B3LYP), and the predicted θ(C−Ge−C) bond angle in the $^3B_1$ state of $Ge(CN)_2$ is considerably larger by (24°) compared to its corresponding neutral ground state $^1A_1$ $Ge(CN)_2$.

For $Ge(CN)_2$ the $EA_{ad(ZPVE)}$, EA_{vert}, and VDE are predicted to be 2.78, 2.76, and 2.80 eV (B3LYP), respectively. The E_{IE} varies from 10.51 (BLYP) to 10.86 eV (B3LYP) and the predicted singlet−triplet splitting values lie between 1.76 (BHLYP) and 2.08 eV (MP2). The singlet−triplet splittings (eV) increase consistently from $C(CN)_2$ (0.52 ± 0.05)[39] to $Si(CN)_2$ (1.39)[70] to $Ge(CN)_2$ (1.76) (BHLYP). The monosubstituted cyanogermylene HGeCN computed at the B3LYP/DZP++ method has a singlet ground state, as does the parent germylene GeH_2.[69] The substitution of a C≡N group to GeH_2 further stabilizes the HGeCN singlet ground state and increases the singlet−triplet energy gap as (in eV): GeH_2 (1.16)[69] < HGeCN (1.46) < $Ge(CN)_2$ (1.85).

ii. The Mixed CNGeCN Structure (Figure 2). For the CNGeCN molecule, a slightly shorter cyano C≡N bond length of 1.172 Å (B3LYP), 1.187 Å (BLYP), 1.156 Å (BHLYP), and 1.195 Å (MP2) is predicted compared to the isocyano bond length. The ϕ(Ge−N≡C) quasi-linear bond angle is larger compared to the ϕ(Ge−C≡N) bond angle by 1.5° (B3LYP). The addition of an extra electron to the asymmetric singlet ground state CNGeCN leads to the predicted Ge−C and Ge−N bond distances lengthening by 0.031 and 0.094 Å, respectively (B3LYP), while the divalent angle decreases by 0.4° (B3LYP). The −N═C: bond length decreases by 0.007 Å (B3LYP), while the C≡N bond length increases by 0.006 Å (B3LYP). No significant changes are noted for the ϕ angles for the $^1A' \rightarrow {}^2A''$ process. For ionization of the neutral ground state to the $CNGeCN^+$ cation, the most significant change in the predicted geometrical parameters is the increase in the θ(N−Ge−C) bond angle of 16° (B3LYP). The ϕ(Ge−N≡C) and ϕ(Ge−C≡N) bond angles increase compared to their corresponding neutral species by 7° and 5° (B3LYP), respectively. The $EA_{ad(ZPVE)}$ values lie between 2.12 eV (MP2) and 2.56 eV (B3LYP). These computed electron affinity values are lower than those for the $Ge(CN)_2$ molecule by 0.22 eV (B3LYP), as shown in Table 1. The CNGeCN molecule has predicted EA_{vert} = 2.49 eV and VDE = 2.63 eV (B3LYP). The E_{IE} is predicted to be lower compared to the $Ge(CN)_2$ isomer for DFT computations and is 10.62 eV compared to 10.53 eV (MP2) for $Ge(CN)_2$. The

dx.doi.org/10.1021/ic301225w | Inorg. Chem. 2012, 51, 12152−12164

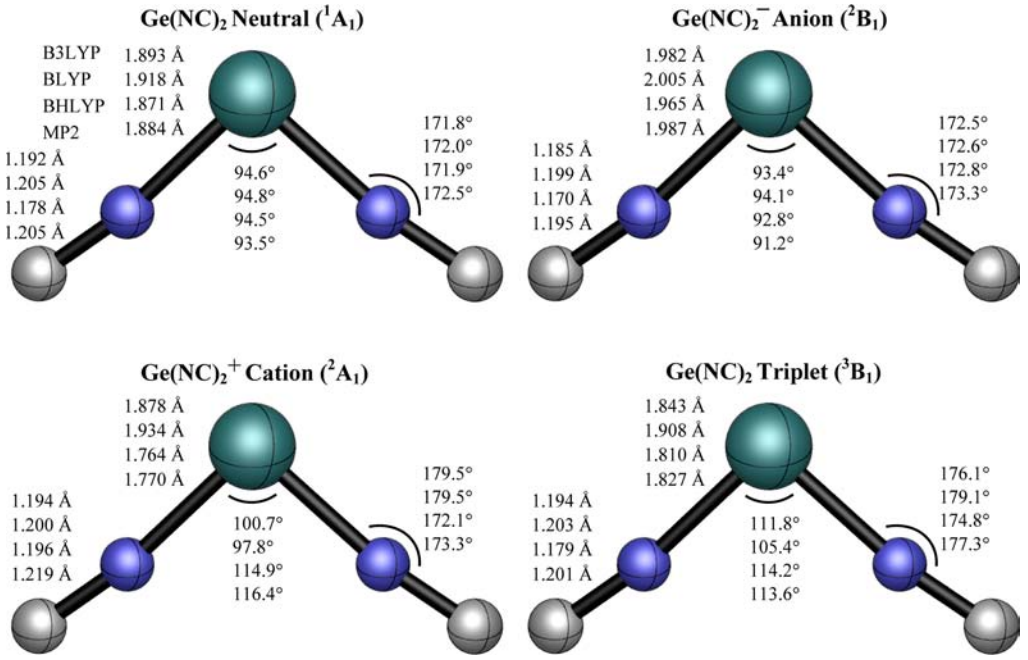

Figure 3. Equilibrium geometries for the $^1A_1$ ground state of $Ge(NC)_2$, $^2B_1$ ground state of the $Ge(NC)_2^-$ anion, $^2A_1$ ground state of the $Ge(NC)_2^+$ cation, and $^3B_1$ excited state of neutral $Ge(NC)_2$.

isocyano group raises ΔE_{S-T} compared to the $Ge(CN)_2$ molecule and the predicted values range from 2.15 (BHLYP) to 2.21 eV (B3LYP).

iii. $Ge(NC)_2$ (Figure 3). The predicted ϕ(Ge−N≡C) angle of the $Ge(NC)_2$ with the B3LYP functional is slightly larger (by 1.3°) compared to the ϕ(Ge−C≡N) bond angle of the $Ge(CN)_2$ molecule. The addition of an extra electron to the neutral $^1A_1$ $Ge(NC)_2$ molecule yields an elongation of the Ge−N bond distances by 0.089 Å, while the −N═C: bond lengths decrease by 0.007 Å (B3LYP). The divalent angle θ decreases slightly by 1.2°, while the ϕ(Ge−N≡C) bond angles increase by 0.7° (B3LYP). The geometrical changes associated with the loss of an electron from the $^1A_1$ neutral $Ge(NC)_2$ species to form the $^2A_1$ $Ge(NC)_2^+$ cation include a decrease in the Ge−N bond lengths of 0.015 Å (B3LYP) and an increase in the N≡C bond lengths of 0.002 Å. The divalent angle increases by 6.1° (B3LYP). The $EA_{ad(ZPVE)}$, EA_{vert}, and VDE at the B3LYP functionals are predicted as 2.32, 2.22, and 2.45 eV, respectively. The E_{IE} ranges from 10.07 eV (BLYP) to 10.82 eV (BHLYP). The singlet−triplet splitting values are larger compared to the $Ge(CN)_2$ species, namely, in the 2.44 eV (BLYP) to 2.63 eV (B3LYP) range.

iv. Cyc_exo_CCN (Figure 4). The neutral $^1A'$ ground state molecule shows a three-membered cyclic system involving dicoordinate Ge and N and tricoordinate C atoms. The $^2A''$ ground state anion has predicted Ge−N, Ge−C, and N═C bond lengths of 2.110, 2.008, and 1.278 Å (B3LYP), respectively, while the angle at Ge decreases compared to its neutral species by nearly 3° (B3LYP). The cationic $^2A'$ cyclic isomer has Ge−N, Ge−C, and N═C bond distances of 1.982 Å, 2.224 Å, and 1.235 Å, respectively, and N−Ge−C divalent angles θ = 33.5° at B3LYP. The exo −C−C≡N bonding of the anionic and cationic species shows slight differences in the bond distances and bond angles compared to the corresponding neutral ground state molecule. In contrast to the bent isomers, the cyclic species display a decrease in the angle at the dicoordinate N by 5.3° (Cyc_exo_CCN) and 4.9° (Cyc_exo_CNC) from the neutral molecule upon electron detachment from the a′ orbital (B3LYP). The Cyc_exo_CCN molecule has a predicted $EA_{ad(ZPVE)}$ = 1.49 eV (B3LYP). A negative electron affinity of $EA_{ad(ZPVE)}$ = −0.71 eV is predicted by the MP2 method. The predicted E_{IE} value with the B3LYP functional is 8.76 eV.

v. Cyc_exo_CNC (Figure 5). The addition of an extra electron to the neutral Cyc_exo_CNC molecule increases the predicted Ge−C and Ge−N bond lengths, whereas the endo N═C bond distance decreases by 0.022 Å with the B3LYP functional. At the MP2 level of computation the Cyc_exo_CNC$^-$ anion is found to lie above its neutral counterpart, similar to the Cyc_exo_CCN molecule. Structural changes are also predicted in going from the neutral Cyc_exo_CNC to its corresponding Cyc_exo_CNC$^+$ cation. The Ge−C bond length increases by 0.288 Å while the Ge−N and C═N bond lengths decrease by 0.002 and 0.049 Å, respectively (B3LYP). The exo C−N bond distance also decreases by 0.063 Å, while the −N═C: bond distance increases by 0.020 Å and the endo Ge−C−N bond angle decreases by 10°. The ease of the Cyc_exo_CNC molecule in adopting an extra electron is predicted to be less than that for the Cyc_exo_CCN species. From Table 1, the $EA_{ad(ZPVE)}$, EA_{vert}, and VDE predictions are 1.43, 1.25, and 1.59 eV, respectively, and E_{IE} is 8.66 eV (B3LYP). Similar to the Cyc_exo_CCN species, a negative $EA_{ad(ZPVE)}$ of −0.74 eV is obtained at the MP2 level.

vi. Linear Triplet NCGeCN, CNGeCN, and CNGeNC Isomers. The fully optimized triplet linear $Ge(CN)_2$, CNGeCN, and $Ge(NC)_2$ isomers are predicted to have one imaginary frequency and are displayed in Figure S2 (Supporting Information). The same trend in the energetic order is maintained as that for their corresponding bent isomers: NCGeCN < CNGeCN < CNGeNC. The predicted energy differences along the series of the linear NCGeCN ⇌ CNGeCN ⇌ CNGeNC are 4.9 and 5.9 kcal mol^{-1} (B3LYP). The linear molecule predicted harmonic imaginary vibrational frequencies at 483*i* [NCGeCN], 328*i* [CNGeCN], and 208*i*

dx.doi.org/10.1021/ic301225w | *Inorg. Chem.* 2012, 51, 12152−12164

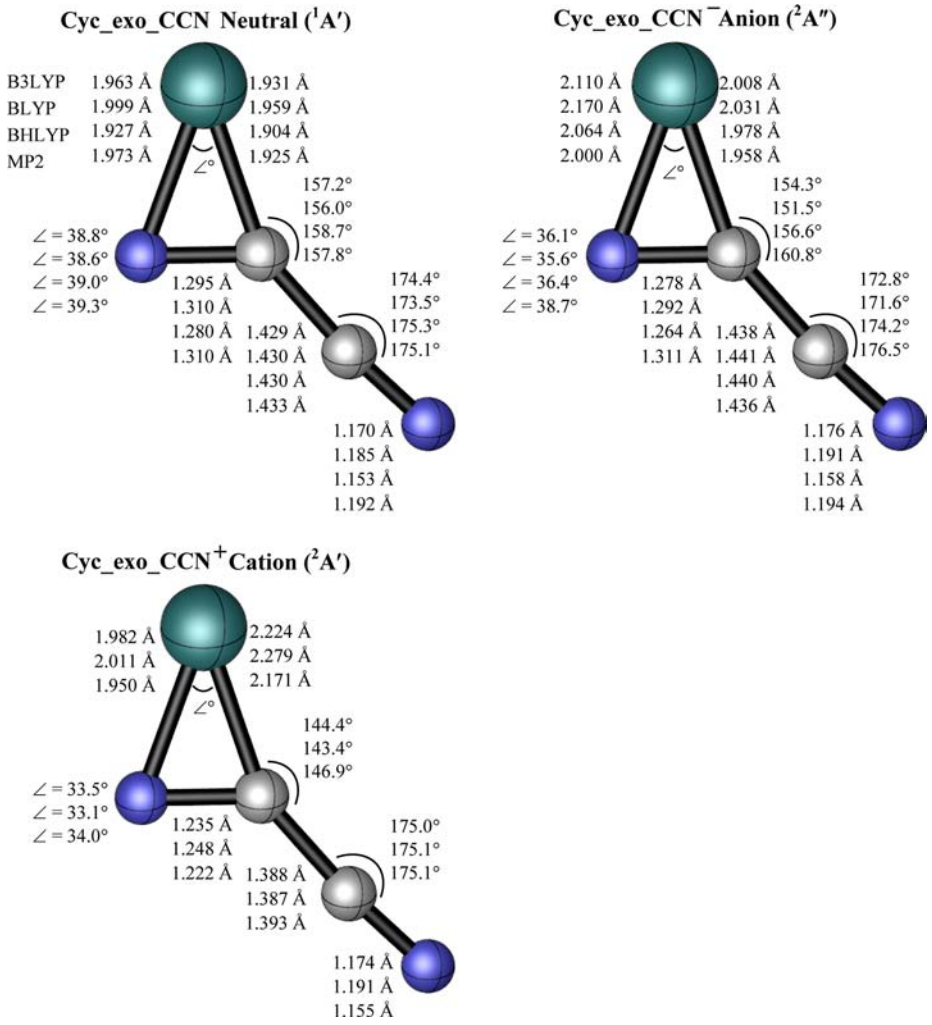

Figure 4. Equilibrium geometries for the ^{1}A′ ground state of Cyc_exo_CCN, ^{2}A″ ground state of the Cyc_exo_CCN$^-$ anion and ^{2}A′ ground state of the Cyc_exo_CCN$^+$ cation.

[CNGeNC] mainly represent the bending modes of the C−Ge−C, N−Ge−C, and N−Ge−N moieties. The barriers to linearity from the lowest-lying bent triplet structures are at 32.3, 26.7, and 22.1 kcal mol^{-1}. In contrast, for the analogous carbene Maier et al.[42] have shown that the valence isoelectronic NCCCN molecule is linear in its triplet ground state.

B. Harmonic Vibrational Frequencies, Infrared Intensities, Raman Activities, Dipole Moments, and Rotational Constants. Tables S3−S7 (Supporting Information) collect the harmonic vibrational frequencies (cm^{-1}), infrared intensities (IR) (km mol^{-1}), and Raman scattering activities (Å^4 amu^{-1}) for the five GeC_2N_2 ground state isomers. For comparison the experimental harmonic vibrational frequency of the diatomic X $^2\Sigma^+$ CN is 2068.6 cm^{-1}.[71] The CN/NC stretching frequencies for the neutral ground states $Ge(CN)_2$, CNGeCN, and $Ge(NC)_2$ isomers are higher than the diatomic CN frequency.

The singlet ground state of $Ge(CN)_2$ is predicted to have strong C≡N stretching vibrational modes predicted at 2229 cm^{-1} (symmetric) and 2227 cm^{-1} (antisymmetric). The less intense Ge−C stretching vibrations are 475 cm^{-1} (symmetric) and 443 cm^{-1} (antisymmetric) with the B3LYP functional. The vibrational frequencies/IR intensities [cm^{-1}/(km mol^{-1})] for singlet ground states CNGeCN = 2087/508 (A′) and $Ge(NC)_2$ = 2080/754 (B_2) are remarkably strong among the nine active vibrational modes, since they belong to the antisymmetric −N═C: stretching motion.

The ^{1}A′ CNGeCN isomer is characterized by C≡N stretching vibrations at 2232 and 2087 cm^{-1} (very strong) with corresponding IR intensities at 71 and 508 km mol^{-1}, while the predicted Ge−N and Ge−C stretches are at 494 and 451 cm^{-1}. The higher C≡N stretching frequency of the Ge−C≡N component reflects the slightly shorter C≡N bond length of 1.172 Å compared to the N≡C distance of 1.192 Å of the Ge−N≡C moiety.

The $^1A_1$ neutral ground state $Ge(NC)_2$ is predicted to have −N═C: strong stretching vibrational modes at 2104 cm^{-1} (symmetric) and 2080 cm^{-1} (antisymmetric), as well as symmetric and antisymmetric stretching vibrations of the isocyano groups at 501 and 469 cm^{-1}, respectively. The dominant harmonic frequencies have respective IR intensities of 278 and 754 km mol^{-1}. Tables S8 and S9 (Supporting Information) present the dipole moments (Debye) and rotational constants (MHz) for ground state $Ge(CN)_2$, CNGeCN, $Ge(NC)_2$, Cyc_exo_CCN, and Cyc_exo_CNC isomers. The magnitude of the dipole moments (Debye) predicted at the B3LYP functional for the different isomers compared to the C_{2v} GeH_2 molecule is GeH_2 (0.22) < CNGeCN (4.19) < Cyc_exo_CNC (4.24) < $Ge(NC)_2$ (4.40) < $Ge(CN)_2$ (4.54) < Cyc_exo_CCN (4.57).

dx.doi.org/10.1021/ic301225w | Inorg. Chem. 2012, 51, 12152−12164

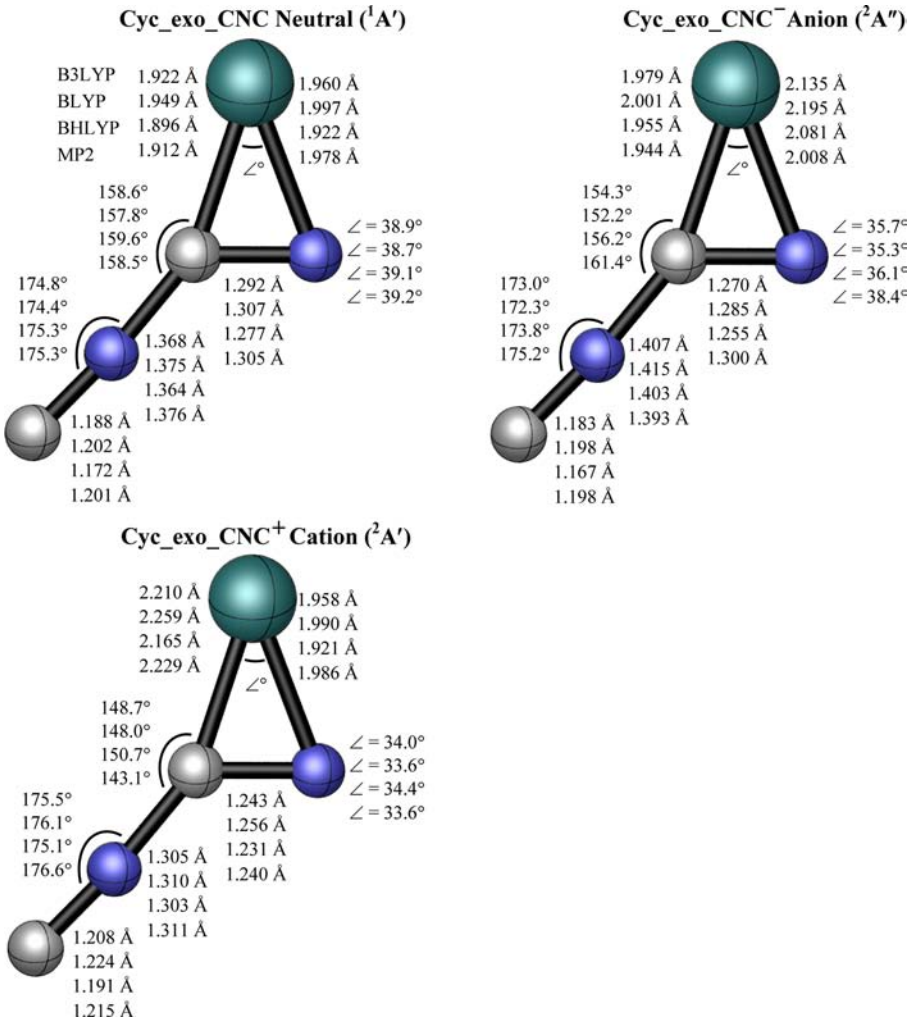

Figure 5. Equilibrium geometries for the ^{1}A′ ground state of Cyc_exo_CNC, ^{2}A″ ground state of the Cyc_exo_CNC$^-$ anion, and ^{2}A′ ground state of the Cyc_exo_CNC$^+$ cation.

C. Isomerization Pathways for the Singlet and Triplet Dicyanogermylenes. There are five minima (three bent and two cyclic isomers) and eight transition states (TSs) including two mirror image conformers on the singlet PES, while on the triplet PES three minima, and four TSs are found. Schematic representations for the unimolecular isomerization pathways of the GeC_2N_2 isomers on the singlet and triplet PESs are displayed in Figures 6 and S3 (Supporting Information), respectively. The PESs include the reactions and twelve TSs indicated in brackets shown in Table 2.

All associated TS structures are non planar. It is predicted that the $Ge(CN)_2 \rightleftharpoons Ge(NC)_2$ interconversion does not occur as a one-step reaction. The lowest energy mechanism involves the formation of the bent isomers via rotation of the cyano groups through the important CNGeCN intermediate. The $Ge(CN)_2 \rightleftharpoons Ge(NC)_2$ interconversion is a two-step process in which the CNGeCN molecule is an intermediate appearing both on the singlet and triplet PESs. The possible rearrangements involving the cyclic isomers are indirect routes on the singlet PES. The more energetic cyclic pathways involve a two-step mechanism comprised of ring closure and ring-opening processes leading to the formation of the mixed CNGeCN isomer.

The theoretical harmonic vibrational frequencies (cm^{-1}) for all located TSs and ZPVE (kcal mol^{-1}) are given in Table S10 (Supporting Information). For all interconversions, we report activation energies including zero-point corrections, E_a, the Gibbs free energy barriers (ΔG), the enthalpies of reactions ΔH (kcal mol^{-1}) at 298.15 K for the singlet and triplet isomerization pathways in Table S11 (Supporting Information). Figure 7 gives a schematic representation of the arbitrary reaction coordinates for the rearrangements of the singlet and triplet isomerization pathways. Figure S4 (Supporting Information) presents all transition states located on the singlet and triplet PESs.

i. Reaction 1a: $Ge(CN)_2 \rightleftharpoons$ CNGeCN. Singlet PES. The TS_1a_S structure is observed to be significantly bent at the $Ge-C_1-N_3$ moiety. The imaginary frequency normal mode predicted at 309*i* cm^{-1} involves primarily the rotation of the reactive cyano group (clockwise or counter-clockwise) toward the divalent germanium center Ge to form the new isocyano group. This mode corresponds to the breakage of the $Ge\cdots C_1$ bond and the formation of a stretched $Ge-N_3$ bond. The $Ge\cdots C_1$ bond being broken is lengthened by 0.243 Å compared to the isolated $^1A_1$ $Ge(CN)_2$. The bond elongation corresponds to 12% of its original length. The quasi-linear bond angle $\phi(Ge-C_1-N_3)$ = 170° for the $^1A_1$ singlet ground state $Ge(CN)_2$ decreases significantly to an acute angle of 71° in TS_1a_S. The $Ge-N_3$ bond being formed in TS_1a_S has a predicted bond length 2.168 (B3LYP) or 2.121 Å (MP2).

dx.doi.org/10.1021/ic301225w | Inorg. Chem. 2012, 51, 12152−12164

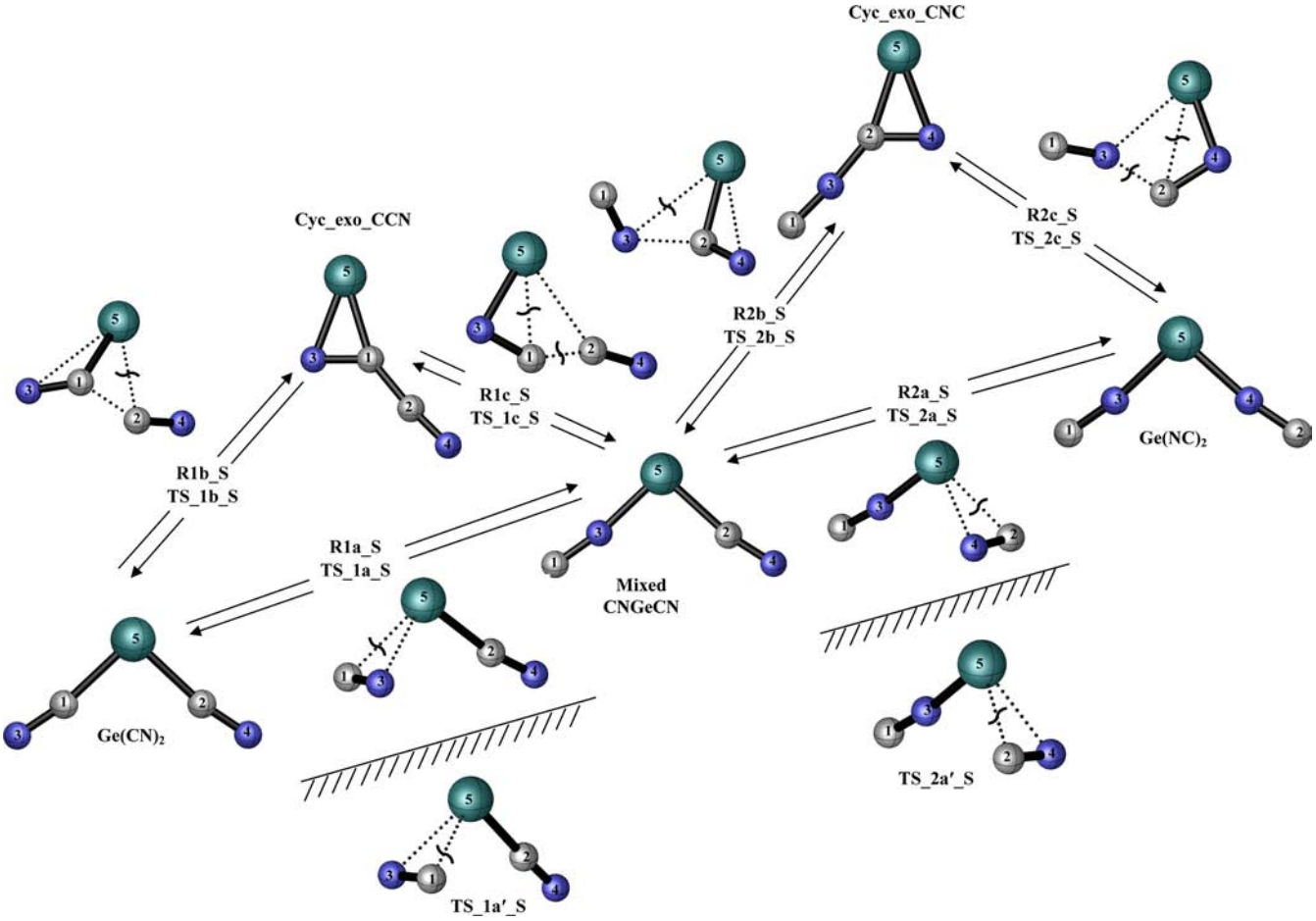

Figure 6. Schematic representations for the unimolecular isomerization pathways of the GeC_2N_2 isomers on the singlet PESs.

Table 2. Representation of Reactions on the Singlet and Triplet PESs and their TSs

singlet potential energy surface	
R1a_S: $Ge(CN)_2 \rightleftharpoons$ CNGeCN	[TS_1a_S and mirror image denoted as TS_1a′_S]
R1b_S: $Ge(CN)_2 \rightleftharpoons$ Cyc_exo_CCN	[TS_1b_S]
R1c_S: Cyc_exo_CCN $\rightleftharpoons$ CNGeCN	[TS_1c_S]
R2a_S: CNGeCN $\rightleftharpoons$ $Ge(NC)_2$	[TS_2a_S and mirror image denoted as TS_2a′_S]
R2b_S: CNGeCN $\rightleftharpoons$ Cyc_exo_CNC	[TS_2b_S]
R2c_S: Cyc_exo_CNC $\rightleftharpoons$ $Ge(NC)_2$	[TS_2c_S]
triplet potential energy surface	
R1a_T: $Ge(CN)_2 \rightleftharpoons$ CNGeCN	[TS_1a_T and TS_1a_$\mathbb{T}$]
R2a_T: CNGeCN $\rightleftharpoons$ $Ge(NC)_2$	[TS_2a_T and TS_2a_$\mathbb{T}$]

There are no significant changes for the $Ge-C_2$, C_2-N_4 bond lengths and the $\phi(Ge-C_2-N_4)$ quasi-linear bond angle. The $Ge(CN)_2 \rightleftharpoons$ CNGeCN isomers interconvert via an activation energy, E_a = 17.5 kcal mol^{-1} (B3LYP), and reaction R1a_S is endothermic, ΔH = +2.3 kcal mol^{-1}.

Triplet PES. From the excited $^3B_1$ $Ge(CN)_2$ to TS_1a_T the rotating C≡N moiety is found to be almost perpendicular to the C_1-Ge-C_2 plane, forming a three-membered cyclic system containing the C_1, Ge, and N_3 atoms. The $Ge\cdots C_1$ bond being broken in TS_1a_T is lengthened by 0.104 Å, accounting for a 5% increase compared to the $Ge-C_1$ bond length of its corresponding symmetric $^3B_1$ $Ge(CN)_2$ reactant. Similar to the singlet PES for the $Ge(CN)_2 \rightleftharpoons$ CNGeCN isomerization, no significant changes are noted for the $Ge-C_2$ and C_2-N_4 bond distances and the $\phi(Ge-C_2-N_4)$ bond angle. The harmonic imaginary frequencies for TS_1a_T and TS_1a_$\mathbb{T}$ structures are predicted to be 246*i* and 202*i* cm^{-1}, representing the rotating motion of the cyano group with the dipole vector directed toward the Ge atom in concert with the stretching mode of the $Ge\cdots C_1$ bond. The favorable pathway is through the TS_1a_$\mathbb{T}$ structure, compared to TS_1a_T by 1.6 kcal mol^{-1}. The predicted E_a (kcal mol^{-1}) for the reactions R1a_T passing through TS_1a_T and TS_1a_$\mathbb{T}$ are 22.5 and 20.9, respectively, while ΔH = 10.5 kcal mol^{-1}.

ii. Reaction 1b: $Ge(CN)_2 \rightleftharpoons$ Cyc_exo_CCN. In constructing the singlet PES for the interconversion of the GeC_2N_2 isomers, a three-membered [Ge, C, N] cyclic system, with exocyclic −C−C≡N bonding has been located. This is represented in pathway R1b_S, which proceeds toward the lowest energy Cyc_exo_CCN isomer. The motion corresponding to the

dx.doi.org/10.1021/ic301225w | *Inorg. Chem.* 2012, 51, 12152−12164

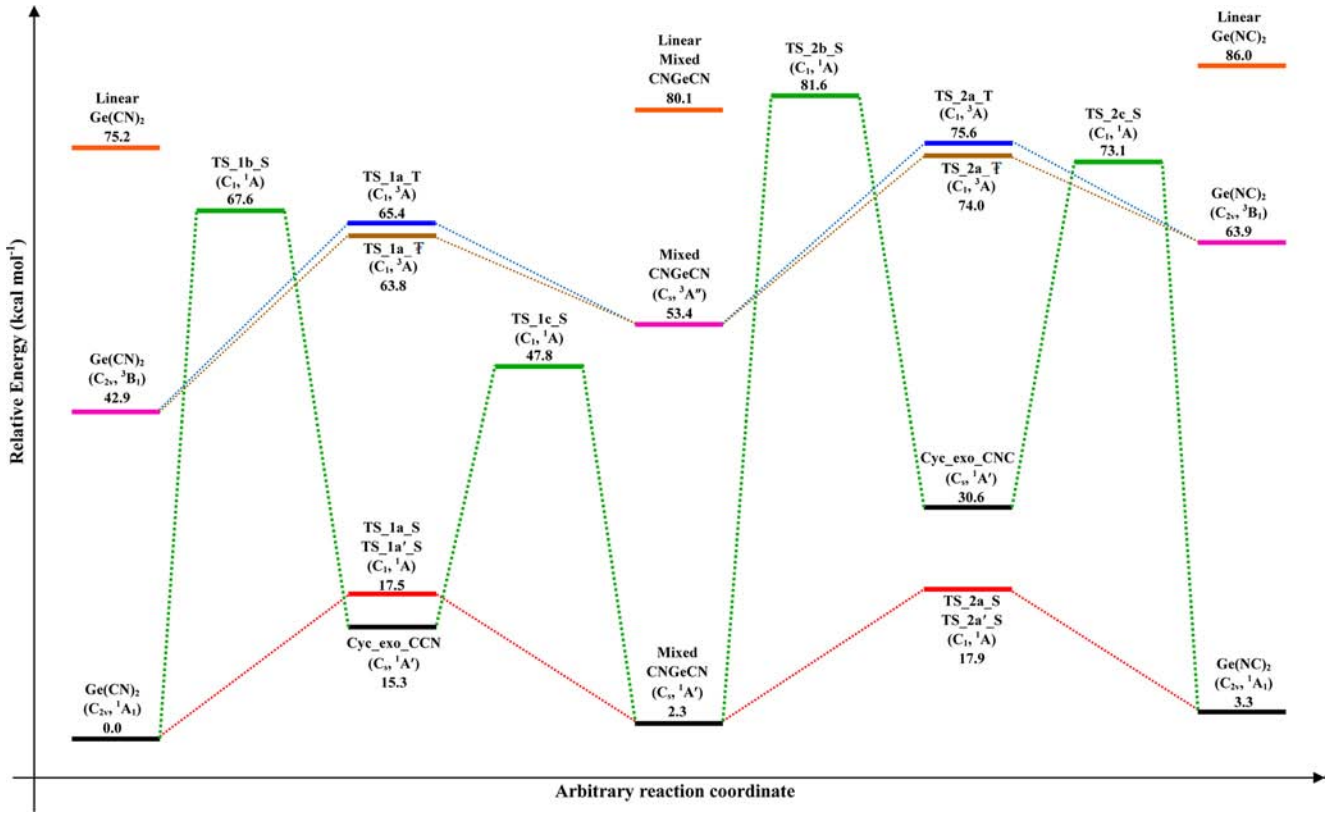

Figure 7. Arbitrary reaction coordinates (kcal mol^{-1}) for the $Ge(CN)_2$, CNGeCN, $Ge(NC)_2$, Cyc_exo_CCN, and Cyc_exo_CNC isomers. Relative energies are obtained using the B3LYP optimized geometries corrected by the addition of ZPVE.

harmonic imaginary vibrational frequency of 285*i* cm^{-1} involves the breaking of the Ge···C_2 bond and the concerted formation of the bonds between Ge and N_3 and between C_1 and C_2. This involves a major rearrangement of the atoms, to produce the cyclic isomer with an exo C−C≡N group. The Ge···C_2 bond being broken is elongated by 0.53 Å, corresponding to a bond elongation of 27%. The newly formed C_1−C_2 bond appears in a three-membered ring structure with an exocyclic −C≡N moiety. The bond formed between Ge and N_3 is predicted to be 2.427 (MP2) or 2.663 Å (BHLYP), and the C_1−N_3 bond is nearly perpendicular to the germylene center. The ring closure in TS_1b_S proceeds through an activation energy, E_a = 67.6 kcal mol^{-1}. The activation energy for this cyclization process is predicted to be high, partly because of the steric strain of the three membered [Ge, N, C] ring with its small interior bond angles and also due to the extensive electronic reorganization that takes place. The TS_1b_S structure leads to the ^{1}A′ Cyc_exo_CCN product; the process is endothermic by 15.3 kcal mol^{-1}.

iii. Reaction 1c: Cyc_exo_CCN ⇌ CNGeCN. The interconversion of the isomers Cyc_exo_CCN ⇌ CNGeCN involves a ring-opening step approaching a four-membered Ge−N_3−C_1−C_2 cyclic system. The reaction proceeds toward TS_1c_S, with the concerted breaking of the Ge···C_1 and C_1···C_2 bonds and the formation of the new Ge−C_2 bond. The harmonic imaginary frequency associated with TS_1c_S, 225*i* cm^{-1} corresponds to the lengthening of the Ge−C_1 and C_1−C_2 bonds, with the C_2 of the cyano group approaching the divalent germanium atom. Along the singlet PES, the Ge−C_1 distance in TS_1c_S is lengthened with respect to Cyc_exo_CCN by 0.26 Å corresponding to a bond elongation of 13%. The reorganization of the atoms from the cyclic system to the bent CNGeCN isomer which comprises the ring-opening step is relatively low compared to ring closure pathway R1b_S. The Ge−C_2 and C_2−N_4 bond lengths decrease by 0.505 Å and 0.021 Å, respectively, while the Ge−C_2−N_4 bond angle increases by 29° on the pathway R2c_S in yielding the CNGeCN molecule. The ϕ(Ge−C_2−N_4) bond angle of TS_1c_S increases considerably from 141° to form the quasi-linear bond angle of 170° in the singlet ground state intermediate CNGeCN. The Ge−N_3−C_1 bond angle opens from 84.0° in the TS to a quasi-linear bond angle of 171.6° for CNGeCN. The Cyc_exo_CCN ⇌ CNGeCN reaction requires an E_a = 32.5 kcal mol^{-1}, while the enthalpy change for the process is exothermic by ΔH = −13.0 kcal mol^{-1}. Hence, the indirect route forms a double-hump on the arbitrary reaction coordinate.

iv. Reaction 2a: CNGeCN ⇌ Ge(NC)$_2$. Singlet PES. The reaction pathway R2a_S on the singlet PES takes place through TS_2a_S with an imaginary frequency of 298*i* cm^{-1}. There are significant changes in the geometry at the Ge−C_2−N_4 moiety from the reactant as it approaches the TS structure. The breaking Ge···C_2 bond distance lengthens by 0.22 Å representing an increase of 11%. The C−N bond distance increases by only 1.4% of its original bond length. The quasi-linear bond angle of the CNGeCN reactant decreases considerably from 170° [CNGeCN] to 72° [TS_2a_S]. The imaginary frequency of 298*i* cm^{-1} corresponds to the rotating motion of the C≡N moiety, where the N atom becomes newly bonded to the divalent germanium atom. The Ge−N_3−C_1 moiety at TS_2a_S is found to be unchanged compared to the reactant and the final product $Ge(NC)_2$. No direct isomerization pathway for the symmetric $Ge(CN)_2$ ⇌ $Ge(NC)_2$ reaction is found on the singlet and triplet PESs; rather

dx.doi.org/10.1021/ic301225w | *Inorg. Chem.* 2012, 51, 12152−12164

CNGeCN acts as an important intermediate between the two isomers. For the CNGeCN ⇌ $Ge(NC)_2$ step the predicted E_a is 15.6 kcal mol^{-1}, and there is a small difference in the energies of the CNGeCN isomer and the $Ge(NC)_2$ product, leading to the predicted endothermicity for the conversion of CNGeCN to $Ge(NC)_2$ of only 1.0 kcal mol^{-1}.

The above findings bring to mind the year 2000 research of Bowie and co-workers.[72] They reported an unusual rearrangement of neutral NC_3N from a joint experimental (mass spectrometric) and theoretical study, indicating that carbon scrambling occurs within the excited singlet state CNCCN via the intermediacy of a four-membered C_{2v}-symmetrical transition structure.

Triplet PES. The ($^3A''$) CNGeCN ⇌ ($^3B_1$) $Ge(NC)_2$ interconversion, through TS_2a_T and TS_2a_T, reveals a major difference compared to the reaction occurring on the singlet PES. The harmonic imaginary frequencies are 275*i* and 232*i* cm^{-1}, respectively, representing the stretching mode of the Ge−C_2 bond. The Ge···C_2 bond being broken in TS_2a_T is lengthened by 0.11 Å which amounts to an elongation of 6%. The C_2−N_4 group is almost perpendicular to the other Ge−N axis, making an angle of 92° (B3LYP). Subsequently, the C_2−N_4 bond length in TS_2a_T is elongated by 0.02 Å compared to the CNGeCN reactant. The rotation of the C_2−N_4 bond shows that the length of the new bond formed between Ge and atom N_4 is 2.374 Å for TS_2a_T. Study of both TS structures shows that there are no significant changes in the Ge−N_3−C_1 moiety compared to the $^3A''$ CNGeCN molecule. In the lower energy TS_2a_T structure, the N_4−C_2 moiety is located at an angle of 48° (B3LYP) to the Ge_5−C_2 axis. The C_2−N_4 bond length is predicted to increase by nearly 0.036 Å. The new Ge−N_4 bond is almost formed, with a bond length of 1.921 Å for TS_2a_T. The predicted E_a (kcal mol^{-1}) are 22.2 (through TS_2a_T) and 20.6 (through TS_2a_T), while the reactions are endothermic by 10.5 kcal mol^{-1}.

v. Reaction 2b: CNGeCN ⇌ Cyc_exo_CNC. Let us consider the alternative route for the isomerization CNGeCN ⇌ $Ge(NC)_2$, the combined reactions R2b_S and R2c_S. These reactions appear only on the singlet PES. The R2b_S route proceeds through the formation of the singlet ground state cyclic isomer Cyc_exo_CNC, the most highly energetic isomer on the reaction coordinate. The reaction R2b_S progresses through an extensive rearrangement of the atoms, starting from the CNGeCN intermediate moving to the three-membered Cyc_exo_CNC molecule, with exocyclic −C−N≡C bonding. The TS_2b_S structure contains two nearly completely formed, fused three-membered rings. The cyclization takes place through the breakage of the Ge---N_3 bond and the concerted formation of the Ge−N_4 and C_3−C_2 bonds. The Ge−N_3 bond lengthens from 1.888 Å to 2.830 Å in TS_2b_S, a bond elongation of 50%. The Ge−C_2−N_4 moiety is a loosely bonded three-membered ring in which the Ge−N_3 bond is elongated by 1.00 Å. There is a large barrier E_a = 79.3 kcal mol^{-1} (B3LYP) for the CNGeCN ⇌ Cyc_exo_CNC interconversion proceeding via TS_2b_S, while the reaction is significantly endothermic, ΔH = +28.3 kcal mol^{-1}.

vi. Reaction 2c: Cyc_exo_CNC ⇌ Ge(NC)$_2$. This rearrangement involves a four-membered cyclic structure, with a new bond formed between Ge and N_3. The conversion of the three-membered Cyc_exo_CNC to TS_2c_S is a ring-opening process in which the two bonds being broken are N_3−C_2 and Ge−C_2. The imaginary frequency of 335*i* cm^{-1} accounts for the stretching N_3−C_2 bond at the TS. The Ge−C_2 bond in question is elongated by 0.56 Å (29%), while the N_3−C_2 bond is lengthened by 0.15 Å (11%) with the B3LYP functional. The Ge−N_4−C_2 bond angle changes from 69° to 105° in TS_2c_S and opens up to a quasi-linear bond angle of ϕ = 172° in the product structure $Ge(NC)_2$. The N_4=C_2 bond length changes from 1.292 Å in Cyc_exo_CNC to 1.324 Å in TS_2c_S (B3LYP) and decreases to 1.192 Å in the: C=N− bond in the symmetric $Ge(NC)_2$ molecule. Simultaneously, the C_1−N_3 bond length varies from 1.188 Å in Cyc_exo_CNC, to 1.199 Å in the TS and 1.192 Å in the final product. TS_2c_S residing on the ^1A PES results in a barrier E_a = 42.5 kcal mol^{-1}, which is fairly high compared to the energy required for the rearrangement of Cyc_exo_CNC to CNGeCN via TS_1c_S. Reaction 2c is highly exothermic, by ΔH = −27.3 kcal mol^{-1}.

D. Rate Constants. The temperature-dependent rate constants for the isomerization reactions are computed using eqs 6−15 (Supporting Information) via transition state theory. Harmonic vibrational frequency analyses on the optimized structures were used to generate zero-point energies, to be added to the electronic energies to calculate enthalpies (H) at 1 atm and temperatures T = 220, 250, 300, 400, 700, 1000, 2100, and 2500 K. Vibrational partition functions were evaluated within the quantum harmonic approximation. The total partition functions were calculated as a product of the translational, rotational, vibrational, and electronic partition functions[73,74] and the rate coefficients for the reactions can then be determined from transition-state theory. In eq 13, the transmission coefficient κ is used to account for tunneling along the reaction coordinate. The Wigner tunneling correction expressed by eq 13 is attached to the transition-state theory.

In order to check the computed theoretical rate constants in the absence of experimental values, the temperature-dependent rate constants are verified through two approaches. The temperature-dependent rate coefficients for the reactions are determined using eqs 14 and 15. The standard Gibbs free energy change, ΔG in the gas phase, between the TS and reactant was calculated using standard methods of statistical mechanics to evaluate the partition function. The standard Gibbs free energy in the gas-phase is calculated by adding the potential energy to the Gibbs free energy corrections calculated at 1 atm. Tables S12 and S13 (Supporting Information) collect the calculated rate constants (s^{-1}) for all interconversions. The predicted rate constants for the singlet isomerizations of $Ge(CN)_2$ ⇌ CNGeCN and CNGeCN ⇌ $Ge(NC)_2$ in the temperature range of 220−2500 K are (4.7×10^{-5}−2.1×10^{12} s^{-1}) and (1.1×10^{-3}−8.9×10^{11} s^{-1}). Proceeding via the cyclic routes on the singlet PES such as the (R1b_S + R1c_S) and (R2b_S + R2c_S) reactions, the rate constant values are found to be exceptionally low. Figures S5−S8 (Supporting Information) present Arrhenius plots for the GeC_2N_2 isomerizations on the singlet and triplet PESs.

IV. CONCLUSIONS

The structures, neutral-anion energy differences, ionization energies, and singlet−triplet gaps of the $Ge(CN)_2$, CNGeCN, $Ge(NC)_2$, Cyc_exo_CCN, and Cyc_exo_CNC species are predicted. The $EA_{ad(ZPVE)}$ (B3LYP) values are 2.78 eV [$Ge(CN)_2$], 2.56 eV [CNGeCN], 2.32 eV [$Ge(NC)_2$], 1.49 eV [Cyc_exo_CCN], and 1.43 eV [Cyc_exo_CNC]. The singlet−triplet splittings (B3LYP) are: 1.85 eV [$Ge(CN)_2$], 2.21 eV [CNGeCN], and 2.63 eV [$Ge(NC)_2$]. The energetic order of the equilibrium structures is $Ge(CN)_2$ < CNGeCN < $Ge(NC)_2$ < Cyc_exo_CCN < Cyc_exo_CNC. All five isomers

dx.doi.org/10.1021/ic301225w | *Inorg. Chem.* 2012, 51, 12152−12164

are energetically well below the dissociation limit to Ge (^{3}P) + C_2N_2 ($^1\Sigma_g$). The linear $Ge(CN)_2$, CNGeCN, and $Ge(NC)_2$ structures have one imaginary vibrational frequency, in contrast with their carbene and silylene analogues. All cyanogermylenes are predicted to have large dipole moments; hence these compounds should be possible to isolate experimentally. The isomerization pathways are studied on both the singlet and triplet PESs. The major mechanistic conclusion from these computations is that on both the singlet and triplet potential energy surfaces the rearrangements are predicted to involve direct steps $Ge(CN)_2 \rightleftharpoons$ CNGeCN $\rightleftharpoons Ge(NC)_2$ without cyclic intermediates. Another significant prediction is that these are fast reactions in both the forward and reverse directions. Because of the small energy differences, it can be anticipated that equilibria will be established. On the triplet surface, two TSs with different energies are obtained for the $Ge(CN)_2 \rightleftharpoons$ CNGeCN and CNGeCN $\rightleftharpoons Ge(NC)_2$ reactions, respectively. The mechanism involved is mainly a rotation about the cyano group. The appearance of the three-membered cyclic isomers requires a major rearrangement of the atoms. The results obtained from this research may assist in the further experimental characterization of the GeC_2N_2 isomers. Our models estimate that the most favorable reactions passing through the bent structural isomerizations to lie from (4.7×10^{-5}–2.1×10^{12} s^{-1}) for R1a_S and (1.1×10^{-3}–8.9×10^{11} s^{-1}) for R2a_S in the temperature range 220–2500 K.

■ ASSOCIATED CONTENT

Supporting Information

Plots of electrostatic potentials, linear geometries, isomerization of triplet excited states, isomerization of transition states, Arrhenius plots, rate constants, and tables of electronic configurations, NBO population analyses, harmonic vibrational frequencies, infrared intensities, Raman scattering activities, dipole moment, rotational constants, theoretical harmonic vibrational frequencies, theoretical activation energies, Gibbs free energy, enthalpies, and theoretical rate constants. This material is available free of charge via the Internet at http://pubs.acs.org.

■ AUTHOR INFORMATION

Corresponding Author

*E-mail: ramchemi@intnet.mu (P.R.), qc@uga.edu (H.F.S.).

Present Address

[⊥]Department of Chemistry, Faculty of Science, Universiti Teknologi Malaysia, 81310 UTM, Johor, Malaysia.

Notes

The authors declare no competing financial interest.

■ ACKNOWLEDGMENTS

This research has been supported by the Mauritius Tertiary Education Commission. A.B. acknowledges the use of facilities at the Department of Chemistry, Faculty of Science, Universiti Teknologi Malaysia, 81310 UTM, Johor, Malaysia and the Center for Computational Quantum Chemistry at the University of Georgia, Athens, Georgia, U.S. Research at the University of Georgia was supported by the U.S. National Science Foundation, Grant CHE-1054286 and the Washington University, Saint Louis, Missouri, Grant CHE-1213696. We sincerely thank Dr Qiang Hao for skillful assistance. We also thank the editor and reviewers for their helpful comments.

■ REFERENCES

(1) Wasserman, E.; Barash, L.; Yager, W. A. *J. Am. Chem. Soc.* **1965**, *87*, 2075.
(2) Olsen, J. F.; Burnelle, L. *Tetrahedron* **1969**, *25*, 5451.
(3) Botschwina, P.; Flügge, J. *Chem. Phys. Lett.* **1991**, *180*, 589.
(4) Sherrill, C. D.; Schaefer, H. F. *J. Chem. Phys.* **1994**, *100*, 8920.
(5) Ding, Y. H.; Huang, X. R.; Li, Z. S.; Sun, C. C. *J. Chem. Phys.* **1998**, *108*, 2024.
(6) Richardson, N. A.; Yamaguchi, Y.; Schaefer, H. F. *J. Chem. Phys.* **2003**, *119*, 12946.
(7) Zhao, Z.-X.; Hou, C.-Y.; Shu, X.; Zhang, H.-X.; Sun, C.-C. *Theor. Chem. Acc.* **2009**, *124*, 85.
(8) Kiefer, A. M.; Paskiewicz, D. M.; Clausen, A. M.; Buchwald, W. R.; Soref, R. A.; Lagally, M. G. *ACS Nano* **2011**, *5*, 1179.
(9) Karttunen, A. J.; Fässler, T. F.; Linnolahti, M.; Pakkanen, T. A. *Inorg. Chem.* **2011**, *50*, 1733.
(10) Gomopoulos, N.; Saini, G.; Efremov, M.; Nealey, P. F.; Nelson, K.; Fytas, G. *Macromolecules* **2010**, *43*, 1551.
(11) Dendramis, A; Leroi, G. E. *J. Chem. Phys.* **1977**, *10*, 4334.
(12) Stroh, F.; Winnewisser, B. P.; Winnewisser, M.; Reisenauer, H. P.; Maier, G.; Goede, S. J.; Bickelhaupt, F. *Chem. Phys. Lett.* **1989**, *160*, 105.
(13) Kellogg, C. B.; Galbraith, J. M.; Fowler, J. E.; Schaefer, H. F. *J. Chem. Phys.* **1994**, *101*, 430.
(14) Blanch, R. J.; McCluskey, A. *Chem. Phys. Lett.* **1995**, *241*, 116.
(15) Maier, G.; Reisenauer, H. P.; Egenolf, H.; Glatthaar, J. *Eur. J. Org. Chem.* **1998**, 1307.
(16) Nimlos, M. R.; Davico, G.; Geise, C. M.; Wenthold, P. G.; Lineberger, W. C.; Blanksby, S. J.; Hadad, C. M.; Petersson, G. A.; Ellison, G. B. *J. Chem. Phys.* **2002**, *9*, 4323.
(17) Goebbert, D. J.; Velarde, L.; Khuseynov, D.; Sanov, A. *J. Phys. Chem. Lett.* **2010**, *1*, 792.
(18) Saito, S.; Endo, Y.; Hirota, E. *J. Chem. Phys.* **1984**, *4*, 1427.
(19) Scheller, M. K.; Cederbaum, L. S.; Tarantelli, F. *J. Am. Chem. Soc.* **1990**, *112*, 9484.
(20) Huang, M.; Su, M.-D. *J. Organomet. Chem.* **2002**, *659*, 121.
(21) Bernheim, R. A.; Kempf, R. J.; Humer, P. W.; Skell, P. S. *J. Chem. Phys.* **1964**, *41*, 1156.
(22) Harrison, J. F.; Dendramis, A.; Leroi, G. E. *J. Am. Chem. Soc.* **1978**, *100*, 4352.
(23) Zandler, M. E.; Goddard, J. D.; Schaefer, H. F. *J. Am. Chem. Soc.* **1979**, *101*, 1072.
(24) Kim, K. S.; Schaefer, H. F.; Radom, L.; Pople, J. A.; Binkley, J. S. *J. Am. Chem. Soc.* **1983**, *105*, 4148.
(25) Rice, J. E.; Schaefer, H. F. *J. Chem. Phys.* **1987**, *86*, 7051.
(26) Malmquist, P. A.; Lindh, R.; Roos, B. O.; Ross, S. *Theor. Chim. Acta* **1988**, *73*, 155.
(27) Brown, F. X.; Saito, S.; Yammamoto, S. *J. Mol. Spectrosc.* **1990**, *143*, 203.
(28) Seidl, E.; Schaefer, H. F. *J. Chem. Phys.* **1992**, *96*, 4449.
(29) Morter, C. L.; Farhat, S. K.; Curl, R. F. *Chem. Phys. Lett.* **1993**, *207*, 153.
(30) McCarthy, M. C.; Gottlieb, C. A.; Cooksy, A. L.; Thaddeus, P. *J. Chem. Phys.* **1995**, *103*, 7779.
(31) Miller, C. E.; Eckhoff, W. C.; Curl, R. F. *J. Mol. Struct.* **1995**, *352*, 435.
(32) Koput, J. *J. Phys. Chem. A* **2003**, *107*, 4717.
(33) Han, J. X.; Hung, P. Y.; DeSain, J.; Jones, W. E.; Curl, R. F. *J. Mol. Spectrosc.* **1999**, *198*, 421.
(34) Allen, M. D.; Evenson, K. M.; Brown, J. M. *J. Mol. Spectrosc.* **2001**, *209*, 143.
(35) Hung, P. Y.; Sun, F.; Hunt, N. T.; Burns, L. A.; Curl, R. F. *J. Chem. Phys.* **2001**, *115*, 9331.
(36) Blanksby, S. J.; Dua, S.; Bowie, J. H.; Schroder, D.; Schwarz, H. *J. Phys. Chem. A* **2000**, *104*, 11248.
(37) Hoffmann, R.; Zeiss, G. D.; VanDine, G. W. *J. Am. Chem. Soc.* **1968**, *90*, 1485.
(38) Lucchese, R. R.; Schaefer, H. F. *J. Am. Chem. Soc.* **1977**, *99*, 13.

(39) Goebbert, D. J.; Pichugin, K.; Khuseynov, D.; Wenthold, P. G.; Sanov, A. *J. Chem. Phys.* **2010**, *132*, 224301.
(40) Chaudhuri, R. K.; Krishnamachari, S. L. N. G. *J. Phys. Chem. A* **2007**, *111*, 4849.
(41) Hajgató, B.; Flammang, R.; Veszprémi, T.; Nguyen, M. T. *Mol. Phys.* **2002**, *100*, 1693.
(42) Maier, G.; Reisenauer, H. P.; Ruppel, R. *Eur. J. Org. Chem.* **2003**, 2695.
(43) Maier, G.; Reisenauer, H. P. *Eur. J. Org. Chem.* **2005**, 2015.
(44) Bowman, J. M.; Gazdy, B. *J. Phys. Chem. A* **1997**, *101*, 6384.
(45) Dubnikova, F.; Lifshitz, A. *J. Phys. Chem. A* **1998**, *102*, 5876.
(46) Maier, G.; Reisenauer, H. P.; Egenolf, H.; Glatthaar, J. *Eur. J. Org. Chem.* **1998**, 1307.
(47) Decker, B. K.; Macdonald, R. G. *J. Phys. Chem. A* **2001**, *105*, 6817.
(48) Islam, S. M.; Hollett, J. W.; Poirier, R. A. *J. Phys. Chem. A* **2007**, *111*, 526.
(49) Onyszchuk, M.; Castel, A.; Riviere, P.; Satge, J. *J. Organomet. Chem.* **1986**, *317*, C35.
(50) Brown, Z. D.; Vasko, P.; Fettinger, J. C.; Tuononen, H. M.; Power, P. P. *J. Am. Chem. Soc.* **2012**, *134*, 4045.
(51) Hihara, G.; Hynes, R. C.; Lebuis, A.-M.; Rivière-Baudet, M.; Wharf, I.; Onyszchuk, M. *J. Organomet. Chem.* **2000**, *598*, 276.
(52) Gaspar, P. P. In *Reactive Intermediates*; Jones, M., Jr., Moss, R. A., Eds.; Wiley: New York, 1985; Vol. 3, p 333.
(53) Gaspar, P. P.; West, R. In *The Chemistry of Organic Silicon Compounds*; Rappoport, Z, Apeloig, Y., Eds.; John Wiley & Sons Ltd.: Chichester, U.K., 1998; Vol. 2, p 2463.
(54) Grev, R. S.; Schaefer, H. F. *Organometallics* **1992**, *11*, 3489.
(55) Trinquier, G. *J. Am. Chem. Soc.* **1990**, *112*, 2130.
(56) Khabashesku, V. N.; Boganov, S. E.; Antic, D.; Nefedov, O. M.; Michl, J. *Organometallics* **1996**, *15*, 4174.
(57) Lei, D.; Lee, M. E.; Gaspar, P. P. *Tetrahedron* **1997**, *53*, 10179.
(58) Frisch, M. J.; Trucks, G. W.; Schlegel, H. B.; Scuseria, G. E.; Robb, M. A.; Cheeseman, J. R.; Montgomery, J. A., Jr.; Vreven, T.; Kudin, K. N.; Burant, J. C.; Millam, J. M.; Iyengar, S. S.; Tomasi, J.; Barone, V.; Mennucci, B.; Cossi, M.; Scalmani, G.; Rega, N.; Petersson, G. A.; Nakatsuji, H.; Hada, M.; Ehara, M.; Toyota, K.; Fukuda, R.; Hasegawa, J.; Ishida, M.; Nakajima, T.; Honda, Y.; Kitao, O.; Nakai, H.; Klene, M.; Li, X.; Knox, J. E.; Hratchian, H. P.; Cross, J. B.; Bakken, V.; Adamo, C.; Jaramillo, J.; Gomperts, R.; Stratmann, R. E.; Yazyev, O.; Austin, A. J.; Cammi, R.; Pomelli, C.; Ochterski, J. W.; Ayala, P. Y.; Morokuma, K.; Voth, G. A.; Salvador, P.; Dannenberg, J. J.; Zakrzewski, V. G.; Dapprich, S.; Daniels, A. D.; Strain, M. C.; Farkas, O.; Malick, D. K.; Rabuck, A. D.; Raghavachari, K.; Foresman, J. B.; Ortiz, J. V.; Cui, Q.; Baboul, A. G.; Clifford, S.; Cioslowski, J.; Stefanov, B. B.; Liu, G.; Liashenko, A.; Piskorz, P.; Komaromi, I.; Martin, R. L.; Fox, D. J.; Keith, T.; Al-Laham, M. A.; Peng, C. Y.; Nanayakkara, A.; Challacombe, M.; Gill, P. M. W.; Johnson, B.; Chen, W.; Wong, M. W.; Gonzalez, C.; Pople, J. A. *Gaussian 03*, revision C.02; Gaussian, Inc.: Wallingford, CT, 2004.
(59) Becke, A. D. *J. Chem. Phys.* **1988**, *38*, 3098.
(60) Becke, A. D. *J. Chem. Phys.* **1993**, *98*, 1372.
(61) Lee, C.; Yang, W.; Parr, R. G. *Phys. Rev. B* **1988**, *37*, 785.
(62) Møller, C.; Plesset, M. S. *Phys. Rev.* **1934**, *46*, 618.
(63) Reed, A. E.; Curtiss, L. A.; Weinhold, F. *Chem. Rev.* **1988**, *88*, 899.
(64) Huzinaga, S. *J. Chem. Phys.* **1965**, *42*, 1293.
(65) Dunning, T. H.; Hay, P. J. In *Modern Theoretical Chemistry*; Schaefer, H. F., Ed.; Plenum: New York, 1977; Vol. 3, p 1.
(66) Huzinaga, S. *Approximate Atomic Wavefunctions II*; University of Alberta: Edmonton, Alberta, 1971.
(67) Lee, T. J.; Schaefer, H. F. *J. Chem. Phys.* **1985**, *83*, 1784.
(68) Schafer, A.; Horn, H.; Ahlrichs, R. *J. Chem. Phys.* **1992**, *97*, 2571.
(69) Bundhun, A.; Ramasami, P.; Schaefer, H. F. *J. Phys. Chem. A* **2009**, *113*, 8080.
(70) Kalcher, J. *J. Phys. Chem. A* **2005**, *109*, 11437.
(71) Huber, K. P.; Herzberg, G. Constants of Diatomic Molecules. *Molecular Spectra and Molecular Structure*, Vol. *IV*; Van Nostrand Reinhold: New York, 1979.
(72) Blanksby, S. J.; Dua, S.; Bowie, J. H.; Schröder, D.; Schwarz, H. *J. Phys. Chem. A* **2000**, *104*, 11248.
(73) Laidler, K. J.; King, M. C. *J. Phys. Chem.* **1983**, *87*, 2657.
(74) Truhlar, D. G.; Garrett, B. C.; Klippenstein, S. J. *J. Phys. Chem.* **1996**, *100*, 12771.